journal

J. Am. Ceram. Soc., 90 [12] 3992–3997 (2007)
DOI: 10.1111/j.1551-2916.2007.02076.x

Structural Aspects of SBA-1 Cubic Mesoporous Silica Synthesized via a Sol–Gel Process Using a Silatrane Precursor

Walairat Tanglumlert,[‡] Toyoko Imae,[§] Timothy J. White,[¶] and Sujitra Wongkasemjit[†,‡]

[‡]The Petroleum and Petrochemical College, Chulalongkorn University, Bangkok 10330, Thailand

[§]Graduate School of Science and Technology, Keio University, Yokohama 223-8522, Japan

[¶]Materials Science and Engineering, Nanyang Technological University, Singapore

Silatrane prepared from fumed silica and triethanolamine was used as a precursor for SBA-1 synthesis at room temperature using cationic surfactants, derived from alkyltrimethylammonium bromides, C_nTMAB ($n = 14$, 16, and 18), as templates in dilute solutions. The influence of acidity, alkyl chain length of the surfactant, and synthesis temperature was studied. The shape of the SBA-1 crystals was dependent on the alkyl chain length of the surfactant. At a high surfactant concentration and an elevated reaction temperature (50°C), three-dimensionally ordered mesopores were invariably produced. Both X-ray diffraction and transmission electron microscopic results showed characteristics of the three-dimensional cubic structure. Scanning electron microscopic images of SBA-1 indicated the crystalline-like appearance of an octadecahedron (18-hedron) consistent with six square {100} and 12 hexagonal {110} planes with a cubic symmetry. The surface area of the product was as high as 1000–1500 m^2/g with an adsorption volume of 0.6–1.0 cm^3/g.

I. Introduction

Since the discovery of M41S silica, many researchers have concentrated on this new class of mesoporous materials.[1,2] It is well known that SBA-1 is analogous to the cubic assemblage of globular micelles in amphophilic surfactant solutions and has a structure suggested as being a cage type with open windows.[3–5] Generally, SBA-1 mesoporous silica is synthesized using tetraethoxysilane as the silica source and a hexadecyltriethylammonium bromide ($C_{16}TEABr$) template with a large head group under highly acidic conditions.[6,7]

However, SBA-1, as compared with other mesoporous materials, such as MCM-41, FSM-16, and SBA-3,[8] has been concentrated, possibly because many large head groups of surfactants are not commercially available. Kim and Ryoo[3] reported that cubic SBA-1, with good three-dimensional order, could be synthesized using alkyltrimethylammonium chloride (C_nTMACl) as a surfactant, and found that low temperatures were favorable for the formation of a high-quality product. Che *et al.*[9] examined the effect of counter ions on mesophase formation and succeeded in synthesizing highly ordered SBA-1 materials with 54 or 74 facets that assumed cubic $Pm\bar{3}n$ *symmetry* formed through the ordering of mesopore layers with *p6mm* planar symmetry.[10] Subsequently, they found that the mesostructure formation was strongly dependent on the acid concentration and they presented a procedure for synthesizing SBA-1 using hexadecyltrimethylammonium bromide ($C_{16}TMAB$) as the template.[4] Chao *et al.*[11] introduced a new concept to synthesize high-quality SBA-1 mesoporous silica in a dilute solution from commercially available alkyltrimethylammonium surfactant and sodium silicate.

In this study, we introduce silatrane as a silica source for the synthesis of SBA-1. While silatrane has been used successfully as a precursor for the synthesis of microporous[12–15] and mesoporous zeolites[16,17] via sol–gel processes, this paper describes the preparation of remarkably high-quality SBA-1 and the influence of acidity, alkyl chain length of the templates, and temperature on the formation and morphology.

II. Methodology

(1) Materials

The silatrane precursor was synthesized from fumed silica (99.8%, Sigma-Aldrich, St. Louis, MO) and triethanolamine (TEA) (Carlo Erba, Milan, Italy) reactants; ethylene glycol (EG) (J.T. Baker, Philipsburg, NJ) was used as the solvent, and acetronitrile (Labscan, Bangkok, Thailand) as an agent for silatrane purification. Mesoporous SBA-1 was synthesized from the silatrane and C_nTMAB (Sigma-Aldrich) used as the template, with H_2SO_4 and NaOH (Labscan) used as catalysts.

(2) Preparation of Silatrane Precursor

Following the method of Wongkasemjit's group,[18,19] silatrane was synthesized directly by mixing SiO_2 and TEA in a simple distillation set using an EG solvent via the Oxide One Pot Synthesis process. The reaction took place at the boiling point of EG (200°C) under a nitrogen atmosphere to remove water as a by-product, along with the EG, from the system. The reaction was run for 10 h, after which the remaining EG was removed under vacuum at 110°C to obtain a brown solid. The crude product was washed with acetonitrile and dried in a vacuum desiccator before characterization with a Bruker Optics EQUINOX55 Fourier-transform infrared (FT-IR) absorption spectrometer (Karlsruhe, Germany) at a resolution of 2 cm^{-1}, and a DuPont 2950 thermogravimetric analyzer (TGA; Twin Lakes, WI) using a heating rate of 10°C/min from room temperature to 750°C in a nitrogen atmosphere.

The FT-IR bands observed were 3000–3700 cm^{-1} (w, νO–H), 2860–2986 cm^{-1} (s, νC–H), 1244–1275 cm^{-1} (m, νC–N), 1170–1117 cm^{-1} (bs, νSi–O), 1093 cm^{-1} (s, νSi–O–C), 1073 cm^{-1} (s, νC–O), 1049 cm^{-1} (s, νSi–O), 1021 cm^{-1} (s, νC–O), 785 and 729 cm^{-1} (s, νSi–O–C), and 579 cm^{-1} (w, $\nu N \rightarrow Si$). TGA showed one sharp mass loss transition at 390°C and gave an 18.5% ceramic yield, corresponding to $N(CH_2CH_2O)_3Si–OCH_2CH_2–N(CH_2CH_2OH)_2$ (Scheme 1).

(3) Synthesis of Mesoporous SBA-1

The synthesis procedure was as follows: solution A was prepared by adding the required amount of C_nTMAB ($n = 14$, 16,

S. Bhandarkar—contributing editor

Manuscript No. 23137. Received April 25, 2007; approved August 17, 2007.

This research work was financially supported by the Postgraduate Education and Research Program in Petroleum and Petrochemical Technology (ADB) Fund (Thailand), the Ratchadapisake Sompote Fund, Chulalongkorn University, and the Thailand Research Fund (TRF).

[†]Author to whom correspondence should be addressed. e-mail dsujitra@chula.ac.th

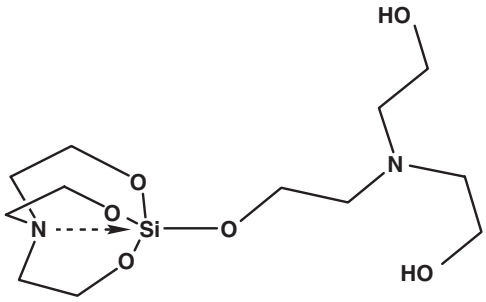

Scheme 1. Structure of silatrane.

and 18) to water (30 mL) and stirring for 0.5 h to obtain a clear solution. Solution B was prepared by adding silatrane (1.4 g, 5 mmol) to 14 mL of H_2SO_4 (0.3–0.5*M*) and NaOH (0.068 g, 1.7 mmol), and stirring for 0.5 h to obtain a homogeneous solution. The pH values of solution B were in the range of 1.5–2 around the isoelectric point (IEP) of silica. Solution B was then added to solution A under vigorous stirring, which was continued for 4 h. Before leaving the mixture at room temperature, water (30 mL) was added to the solution mixture. Then, the mixture was allowed to age for 1–2 days at the desired temperature to form white precipitates. The products were filtered and washed with distilled water and dried overnight in air. Template removal was achieved by calcination at 560°C for 6 h using a Carbolite furnace (CFS 1200, Hope Valley, U.K.) at a heating rate of 0.5°C/min. The mixture composition in molar ratio was $1.0C_n$TMAB:$5SiO_2$:1.7NaOH:xH_2SO_4:$3680H_2O$.

The mesoporous products were characterized using a Rigaku X-ray diffractometer (XRD; Tokyo, Japan) at a scanning speed of 1°/s using Cu$K\alpha$ radiation in the range of $2\theta = 1.5$–8°. SBA-1 morphology was observed by secondary electron imaging with a JEOL 5200-2AE scanning electron microscope (JEOL USA, Peabody, MA), while the mesopore order was directly examined using a JEOL 2010F transmission electron microscope (TEM). The surface area and average pore size were determined by the Brunauer–Emmett–Teller (BET) method with a Quantasorb JR instrument (Mount Holly, NJ).

III. Results and Discussion

SBA-1 mesoporous silica was synthesized using the C_nTMAB with $n = 14$, 16, and 18 as a template in a dilute solution of acid to examine the influence of alkyl chain length on product quality. In addition, acidity and temperature were varied systematically to optimize yield and perfection.

(1) Effect of the Acidity

Because SBA-1 morphology depends on the concentration of acid,[20] the gel composition (C_{16}TMAB:5Si:1.7NaOH:xH_2SO_4:$3680H_2O$) was varied over the range of $x = 0.3$–0.5*M*. Huo *et al.*[6] proposed the formation of the silica–surfactant mesophase under acidic conditions via an $S^+X^-I^+$ pathway at pH <2 or through an $S^+X^-I^o$ pathway at pH = 2 (S, X, and I, correspond to surfactant, halide, and inorganic species, respectively), leading to a variety of topological constructions.[21] In the present case, with the acid concentration varied from 0.3 to 0.5*M*, all samples were well ordered with three distinct XRD peaks at {200}, {210}, and {211} reflections in the range of 1.5°–3°, representing a cubic unit cell with $a = 83$ Å based on the SBA-1 $Pm\bar{3}n$ mesostructure.[22] Other peaks in the higher angle range of 3°–6° indicate a high degree of cubic mesostructured organization. The diffracted intensities declined with increasing concentration of acid. The SBA-1 particles synthesized at 0.5*M* H_2SO_4 were spheres, and those at a decreased acid concentration (0.3*M*) took on an octadecahedral form (Fig. 1). These results are in agreement with the observations of Chao *et al.*,[23] who suggested that the growth of SBA-1 facets could be regarded as a self-assembly process where the surfactant aggregates and silicate species take on specific orientations at particular pH. In dilute acid solutions, the oligosilicate species are isolated and do not condense appreciably, allowing the surfactant aggregates and silicate species to self-assemble in solution and leading to catalyzed silica condensation. Under this condition, being close to the IEP of silica, slow condensation takes place, yielding the differentiation of mesopore surfaces and the formation of cuhedral particles (Fig. 1(a)). At higher pH, the condensation rate accelerates, leading to rapid isotropic growth and anhedral surfaces.

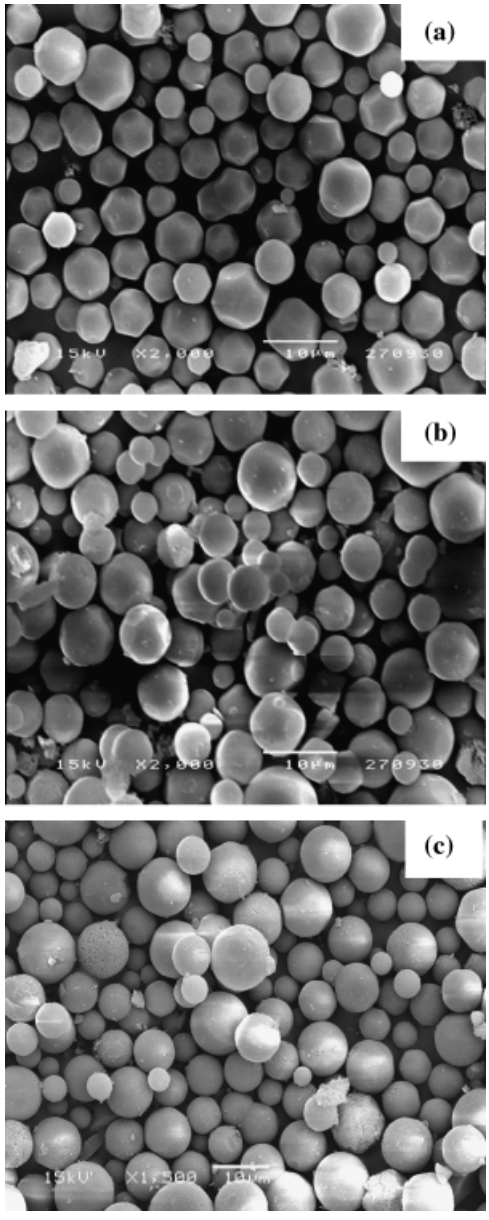

Fig. 1. Scanning electron micrographs of calcined C_{16}TMAB-templated SBA-1 mesoporous silica using different acid concentrations at room temperature; (a) 0.3*M*, (b) 0.4*M*, and (c) 0.5*M* concentration of C_{16}TMAB = 0.04*M*. C_nTMAB, alkyltrimethylammonium bromide.

The external shape of the SBA-1 crystals reflected the perfect mesopore order. TEM images of the products that use 0.3 and 0.5*M* typically showed that domains of regular mesopores were extensive in the latter material (Fig. 2).

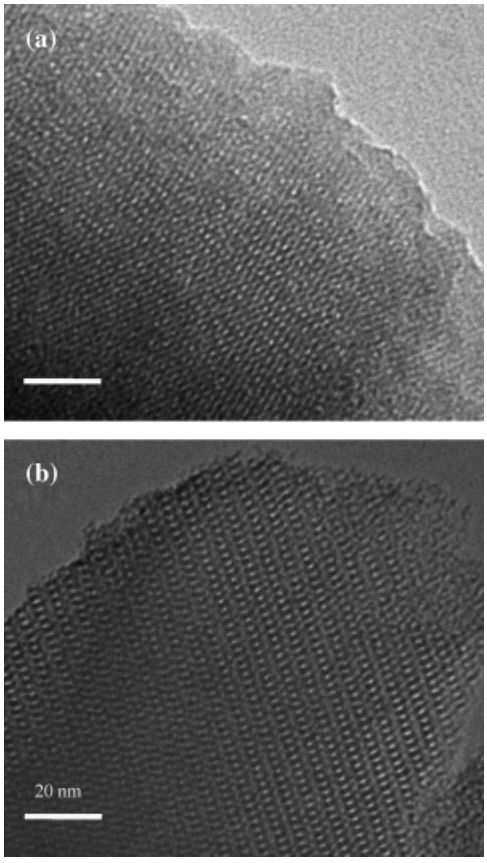

Fig. 2. Transmission electron images of calcined C_{16}TMAB-templated SBA-1 using different acid concentrations at room temperature; (a) 0.3*M* and (b) 0.5*M* concentration of C_{16}TMAB = 0.04*M*. C_nTMAB, alkyltrimethylammonium bromide.

(2) Effect of Alkyl Chain Length in the Surfactant Molecules

For all combinations of C_nTMAB surfactant concentration (0.02–0.06*M*) and alkyl chain length ($n = 14$, 16, and 18) in 0.3*M* H_2SO_4, well-ordered SBA-1 mesoporous silica was obtained. The surfactant having the longest alkyl chain displayed the narrowest diffraction peaks and higher intensity, indicative of a superior long-range mesopore order. However, the diffracted intensities were not significantly altered as a function of surfactant concentration, in agreement with Chao *et al.*[11] These workers found a transformation from a three-dimensionally ordered $Pm\bar{3}n$ phase to a planar structure that retained hexagonal *p6mm* symmetry at a surfactant concentration of 0.06*M*, when using the C_{16}TMAB and C_{18}TMAB as templates. However, the silatrane precursor generating the TEA molecule in the solution allows the space symmetry to be preserved, even at the high template concentration. In addition, the structural order for the cubic mesophase was enhanced by increasing the alkyl chain length because self-assembly is controlled by surfactant hydrophobicity (i.e., chain length) and the concentration.[24] This result can be explained in terms of the concept of surfactant packing parameter, *g*.[6,7] The surfactant packing parameter *g* is given by $g = V/(a_0 l)$, where *V* is the total volume occupied by the alkyl tail group plus any co-solvent organic molecules between the chains, a_0 is the effective head group area at the micelle surface, and *l* is the kinetic length of the alkyl chain. On increasing the chain length, the kinetic length linearly increases along with the volume.[7] However, with TEA molecules penetrating the hydrophilic region, the effective head group (a_0) is expanded. This phenomenon results in a decrease in the *g* value, favoring the $Pm\bar{3}n$ cubic mesophase.

Secondary electron images of SBA-1 templated with C_{14}TMAB, C_{16}TMAB, and C_{18}TMAB surfactants clearly show that the first one with lower hydrophobicity interacts most strongly with the silica species, leading to rapid condensation, smaller particle size, and poorly developed facets (Fig. 3(a)), which is general.[25] For C_{16}TMAB, because the surface energy difference between the {100} and {110} faces is not large, the condensation is slower; thus, octadecahedron crystals are formed.[26] The effect is more pronounced for the C_{18}TMAB material, in which an external octadecahedron (18-hedron) with six square and 12 hexagonal facets is clearly observed,[27,28] possibly as C_{18}TMAB yields more counterion association than both C_{16}TMAB and C_{14}TMAB, leading to an adequate hydrophilic–lipophilic balance (HLB)[21]; the higher hydrophobicity leads to higher counterion condensation and yields better structural ordering in the cubic phase. This means that the longer chain length of the surfactant leads to the higher counterion association, which can promote the formation of larger mesoporous crystals.

The type IV N_2 adsorption–desorption isotherms (Fig. 4) of the calcined SBA-1 templated by C_{14}TMAB to C_{18}TMAB were similar (Table I) and showed a large increase at relative pressure $P/P_0 = 0.2$–0.4 due to the capillary condensation within uniform mesopores.[29,30] The pore size and pore volume of SBA-1 increase with the surfactant chain length. For all products, the surface area is high (1000–1500 m^2/g), with an adsorption volume of 0.6–0.95 cm^3/g.

(3) Effect of Temperature

As liquid crystal formation is affected by temperature, this parameter was thus investigated from room temperature to 50°C and correlated with the structural evolution of SBA-1 during synthesis. At 50°C, C_{16}TMAB- and C_{18}TMAB-templated SBA-1 silica retained the characteristic mesostructure peaks (Figs. 5(B, C)). The former templates can be used to synthesize three-dimensionally ordered structures at a higher temperatures. Kao *et al.*[31] studied the phase control of SBA-1 by the addition of short-chain alcohols, and found that the alcohol additives served as phase controllers at higher temperature. Rationally, as silatrane is a water-soluble alkoxide, the hydrolysis of silatrane to silicate species generates TEA molecules in the solution to act as a cotemplate in mesoporous formation. Because the TEA molecules are branch chain and more hydrophilic, they reside on the outer boundaries of the surfactant micelles, making the surfactant micelles less packed, and reducing the electrostatic repulsion between the head groups. With increasing temperature, the tail motion increases the effective surfactant volume, leading to an increase in the *g* value. However, the confinement of TEA molecules in the hydrophilic region of the surfactants results in an expansion of the effective head group area (a_0), which balances the effect of the surfactant volume (*V*); thus, the *g* value is favored in the formation of the cubic SBA-1 phase.[31–33] In addition, SBA-1 templated by C_{14}TMAB material became less ordered at 50°C (Fig. 5(A)), and it could be synthesized at temperatures lower than 50°C because lower hydrophobic C_{14}TMAB cannot interact strongly with the silica species at a high temperature.

Crystal morphology behavior is also sensitive to temperature. The synthesis at a higher temperature resulted in the formation of a silica–surfactant mesophase with a hexagonal structure.[34–37] Liu *et al.*[38] observed that a phase transformation occurred from three-dimensionally cubic $Pm\bar{3}n$ to two-dimensionally hexagonal *p6mm* while drying the precipitate. However, in our case, we did not observe the phase transformation (not shown), even when the temperature was increased to 50°C. In the case of using C_{14}TMAB, most crystals were octadecahedron, although there were some mosaic-like crystals. For the C_{16}TMAB and C_{18}TMAB, the crystals still had a decahedron shape. This means that the SBA-1 mesoporous silica prepared using the silatrane as a silica source can prevent the morphology change at high temperature because of the generation of TEA molecules as a stabilizer of SBA-1, as discussed above.

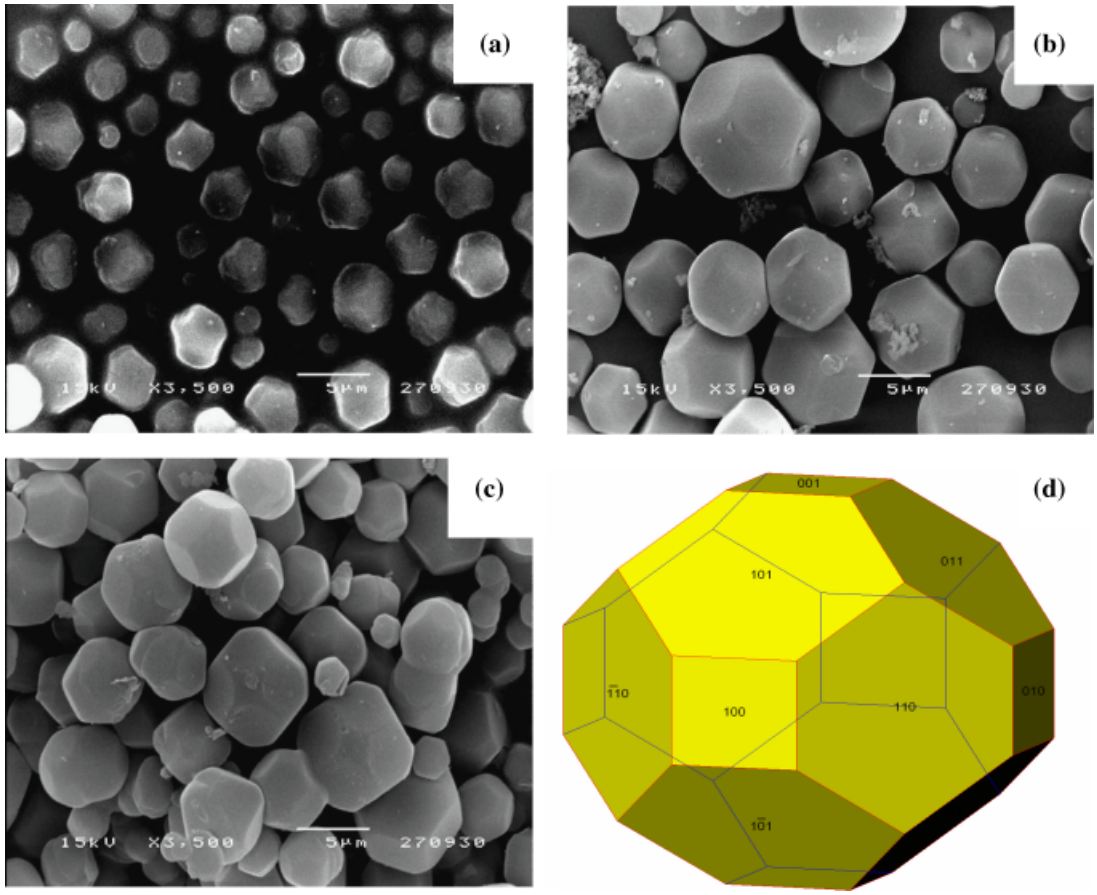

Fig. 3. Scanning electron micrographs of calcined SBA-1 as a function of the alkyl chain length in the surfactant using a surfactant concentration of 0.06 and 0.3*M* H_2SO_4 at room temperature; (a) C_{14}TMAB, (b) C_{16}TMAB, (c) C_{18}TMAB, and (d) a schematic model of the SBA-1 particle with the plane indexes. C_nTMAB, alkyltrimethylammonium bromide.

IV. Conclusions

A silatrane precursor has been successfully used to synthesize well-ordered and stable SBA-1 mesoporous silica via the sol–gel method. Under mild conditions with the small head group of C_nTMAB, high-quality SBA-1 was produced. The TEA molecules generated from the silatrane precursor significantly influenced the structure of the surfactant micelle by decreasing the surfactant packing parameter.

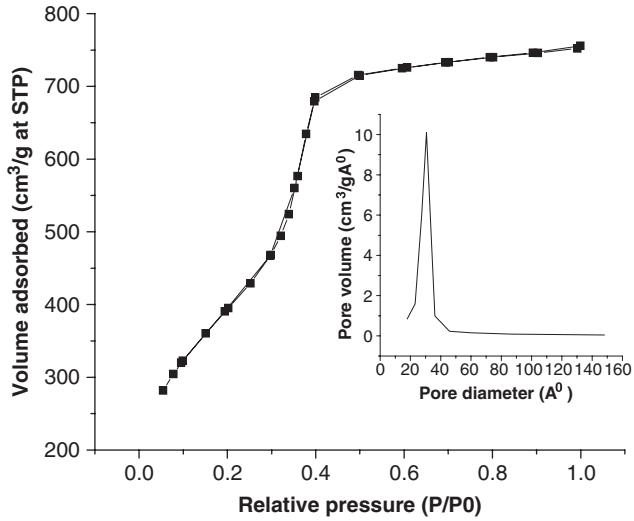

Fig. 4. Nitrogen adsorption–desorption isotherm and pore size distribution plot (inset) of calcined C_{18}TMAB-templated SBA-1 synthesized at room temperature using 0.3*M* H_2SO_4 and 0.06*M* C_{18}TMAB. C_nTMAB, alkyltrimethylammonium bromide.

Table I. BET Analysis of SBA-1 Synthesized at Different Surfactant Concentrations Using 0.3*M* H_2SO_4

Surfactant concentration (*M*)	BET surface area (m^2/g)	Pore volume (cm^3/g)	Average pore size (nm)	d_{210} (nm)	a_0 (nm)†	D_{me} (nm)§
C_{14}TMAB						
0.02	1061	0.50	2.0	3.1	6.9	3.8
0.04	1154	0.60	2.0	3.1	6.9	3.7
0.06	1080	0.65	2.1	3.2	7.2	3.8
C_{16}TMAB						
0.02	1177	0.72	2.1	3.6	8.1	4.6
0.04	1182	0.76	2.1	3.7	8.4	4.7
0.06	1239	0.80	2.1	3.7	8.3	4.7
C_{18}TMAB						
0.02	1297	0.82	2.7	4.3	9.6	5.4
0.04	1435	0.84	2.8	4.4	9.9	5.4
0.06	1520	0.95	2.9	4.4	9.9	5.3

†Lattice parameters a_0 were calculated based on the formula $a_0 = \sqrt{5}d_{210}$. §Cage diameter was determined using the equation $D_{me} = a_0(6\varepsilon_{me}/\pi\nu)^{1/3}$ where D_{me} is the cage diameter of a cubic unit cell of length a_0, ε_{me} is the volume fraction of a regular cavity, and ν ($\nu = 8$, for the SBA-1) is the number of cavities present in the unit cell.[2,29] BET, Brunauer–Emmett–Teller; C_nTMAB, alkyltrimethylammonium bromides.

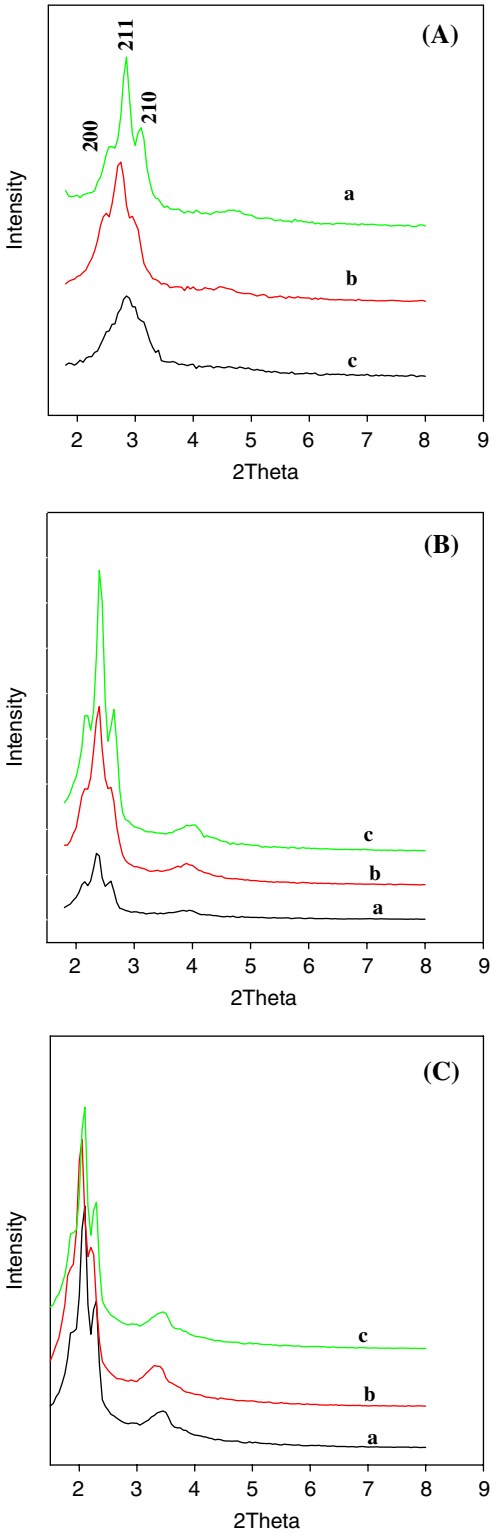

Fig. 5. X-ray diffraction spectra of calcined SBA-1 as a function of the reaction temperature and the alkyl chain length in the surfactant at a concentration of 0.06*M* using 0.3*M* H_2SO_4: (A) C_{14}TMAB, (B) C_{16}TMAB, and (C) C_{18}TMAB, all at (a) room temperature, (b) 40°, and (c) 50°C. C_nTMAB, alkyltrimethylammonium bromide.

References

[1]A. Sayari, "Catalysis by Crystalline Mesoporous Molecular Sieves," *Chem. Mater.*, **8**, 1840–52 (1996).

[2]A. Vinu, V. Murugesan, and M. Hartmann, "Pore Size Engineering and Mechanical Stability of the Cubic Mesoporous Molecular Sieve SBA-1," *Chem. Mater.*, **15**, 1385–93 (2003).

[3]M. J. Kim and R. Ryoo, "Synthesis and Pore Size Control of Cubic Mesoporous Silica SBA-1," *Chem. Mater.*, **11**, 487–91 (1999).

[4]S. Che, Y. Sakamoto, O. Terasaki, and T. Tatsumi, "Synthesis and Morphology Control of SBA-1 Mesoporous Silica with Surfactant of Cetyltrimethylammonium Bromide," *Chem. Lett.*, **2**, 214–5 (2002).

[5]Y. Sakamoto, I. Diaz, O. Terasaki, D. Zhao, J. Perez-Pariente, J. M. Kim, and G. D. Stucky, "Three-Dimensional Cubic Mesoporous Structures of SBA-12 and Related Materials by Electron Crystallography," *J. Phys. Chem. B*, **106**, 3118–23 (2002).

[6]Q. Huo, D. I. Margolese, D. I. Ciesla, D. G. Demuth, P. Feng, T. E. Gier, P. Sieger, A. Firouzi, B. F. Chemelka, F. Schüth, and G. D. Stucky, "Organization of Organic Molecules with Inorganic Molecular Species into Nanocomposite Biphase Arrays," *Chem. Mater.*, **6**, 1176–91 (1994).

[7]Q. Huo, D. I. Margolese, U. Ciesla, D. G. Demuth, P. Feng, T. E. Gier, P. Sieger, A. Firouzi, B. F. Chemelka, and G. D. Stucky, "Surfactant Control of Phases in the Synthesis of Mesoporous Silica-Based Materials," *Chem. Mater.*, **8**, 1147–60 (1996).

[8]D. Ji, T. Ren, L. Yan, and J. Suo, "Synthesis of Ti-Incorporated SBA-1 Cubic Mesoporous Molecular Sieves," *Mater. Lett.*, **57**, 4474–7 (2003).

[9]S. Che, S. Kamiya, O. Terasaki, and T. Tatsumi, "The Formation of Cubic *Pm3n* Mesostructure by an Epitaxial Phase Transformation from Hexagonal *p6mm* Mesophase," *J. Am. Chem. Soc.*, **123**, 12089–90 (2001).

[10]S. Che, S. Lim, M. Kaneda, H. Yoshitake, O. Terasaki, and T. Tatsumi, "The Effect of the Counteranion on the Formation of Mesoporous Materials under the Acidic Synthesis Process," *J. Am. Chem. Soc.*, **124**, 13962–3 (2002).

[11]M. C. Chao, H. P. Lin, D. S. Wang, and C. Y. Tang, "Controlling the Crystal Morphology of Mesoporous Silica SBA-1," *Microporous Mesoporous Mater.*, **83**, 269–76 (2005).

[12]M. Sathupanya, E. Gulari, and S. Wongkasemjit, "ANA and GIS Zeolite Synthesis Directly from Alumatrane and Silatrane by Sol–Gel Process and Microwave Techniques," *J. Eur. Ceram. Soc.*, **22**, 1293–303 (2002).

[13]M. Sathupanya, E. Gulari, and S. Wongkasemjit, "Na-A (LTA) Zeolite Synthesis Directly from Alumatrane and Silatrane by Sol–Gel Microwave Techniques," *J. Eur. Ceram. Soc.*, **23**, 2305–14 (2003).

[14]N. Phonthammachai, T. Chairassameewong, E. Gulari, A. M. Jameison, and S. Wongkasemjit, "Oxide One Pot Synthesis of a Novel Titanium Glycolate and Its Pyrolysis," *J. Met. Mater. Min.*, **12**, 23 (2003).

[15]P. Phiriyawirut, A. M. Jamieson, and S. Wongkasemjit, "VS-1 Zeolite Synthesized Directly from Silatrane," *Microporous Mesoporous Mater.*, **77**, 203–13 (2005).

[16]N. Thanabodeekij, W. Tanglumlert, E. Gulari, and S. Wongkasemjit, "Synthesis of Ti-MCM-41 Directly from Silatrane and Titanium Glycolate and Its Catalytic Activity," *Appl. Organomet. Chem.*, **19**, 1047–54 (2005).

[17]N. Thanabodeekij, S. Sadthayanon, E. Gulari, and S. Wongkasemjit, "Extremely High Surface Area of Ordered Mesoporous MCM-41 by Atrane Route," *Mater. Chem. Phys.*, **98**, 131–7 (2006).

[18]V. Jitchum, C. Sun, S. Wongkasemjit, and H. Ishida, "Synthesis of Spirosilicates Directly from Silica and Ethylene Glycol/Ethylene Glycol Derivatives," *Tetrahedron*, **57**, 3997–4003 (2001).

[19]W. Charoenpinijkarn, M. Suwankruhasn, B. Kesapabutr, S. Wongkasemjit, and A. M. Jamieson, "Sol–Gel Processing of Silatranes," *Eur. Polym. J.*, **37**, 1441–8 (2001).

[20]P. Srinivasu, S. H. Lim, Y. Kubota, and T. Tatsumi, "Synthesis of Highly Ordered Mesoporous $P6_3/mmc$ and *p6mm* Phases by Adding Alcohols to the System for the SBA-1 Synthesis," *Cat. Today*, **117**, 220–7 (2006).

[21]H. P. Lin, C. P. Kao, C. Y. Mou, and S. B. Liu, "Counterion Effect in Acid Synthesis of Mesoporous Silica Materials," *J. Phys. Chem. B*, **104**, 7885–94 (2000).

[22]M. W. Anderson, C. C. Egger, G. J. T. Tiddy, J. L. Casci, and K. A. Brakke, "A New Minimal Surface and the Structure of Mesoporous Silicas," *Angew. Chem. Int.*, **44**, 3243–8 (2005).

[23]M. C. Chao, D. S. Wang, H. P. Lin, and C. Y. Mou, "Control of Single Crystal Morphology of SBA-1 Mesoporous Silica," *J. Mater. Chem.*, **13**, 2853–4 (2003).

[24]K. Holmberg, B. Jonsson, B. Kronberg, and B. Lindan, *Surfactants and Polymers in Aqueous Solution.* Wiley, London, 2002.

[25]M. C. Chao, H. P. Lin, D. S. Wang, and C. Y. Mou, "Synthesis of SBA-1 Mesoporous Silica Crystals with Tunable Pore Size Using Sodium Silicate and Alkyltrimethylammonium Surfactants," *Chem. Lett.*, **33**, 374–5 (2004).

[26]H. P. Lin and C. Y. Mou, "Structural and Morphological Control of Cationic Surfactant-Templated Mesoporous Silica," *Acc. Chem. Res.*, **35**, 927–35 (2002).

[27]S. Guan, S. Inagaki, T. Ohsuna, and O. Terasaki, "Cubic Hybrid Organic–Inorganic Mesoporous Crystal with a Decaoctahedral Shape," *J. Am. Chem. Soc.*, **122**, 5660–1 (2000).

[28]S. Guan, S. Inagaki, T. Ohsuna, and O. Terasaki, "Hybrid Ethane–Siloxane Mesoporous Materials with Cubic Symmetry," *Microporous Mesoporous Mater.*, **44–5**, 167–72 (2001).

[29]H. M. Kao, J. D. Wu, C. C. Cheng, and A. S. T. Chiang, "Direct Synthesis of Vinyl-Functionalized Cubic Mesoporous Silica SBA-1," *Microporous Mesoporous Mater.*, **88**, 319–28 (2006).

[30]H. M. Kao and C. C. Cheng, "Tetramethoxysilane as a Convenient Silicon Source for Phase Control of Cubic SBA-1 Mesostructures," *Mater. Lett.*, **60**, 2594–9 (2006).

[31]H. M. Kao, C. C. Cheng, C. C. Ting, and L. Y. Hwang, "Phase Control of Cubic SBA-1 Mesostructures via Alcohol-Assisted Synthesis," *J. Mater. Chem.*, **15**, 2989–92 (2005).

[32]M. S. Morey, A. Davidson, and G. D. Stucky, "Silica-Based, Cubic Mesostructures: Synthesis, Characterization and Relevance for Catalysis," *J. Porous Mater.*, **5**, 195–204 (1998).

[33]H. M. Kao, Y. W. Liao, and C. C. Ting, "Synthesis of Cubic Mesoporous Silica SBA-1 with Bulky Headgroup Surfactant Cetyltripropylammonium Bromide," *Microporous Mesoporous Mater.*, (2006), in press.

[34]M. Ogura, H. Miyoshi, S. P. Naik, and T. Okubo, "Investigation on the Drying Induced Phase Transformation of Mesoporous Silica: A Comprehensive Understanding toward Mesophase Determination," *J. Am Chem. Soc.*, **126**, 10937–44 (2004).

[35]S. Che, Y. Sakamoto, H. Yoshitake, O. Terasaki, and T. Tatsumi, "The Structure and Morphology Control of Mesoporous Silica under Acidic Conditions," *Microporous Mesoporous Mater.*, **85**, 207–18 (2005).

[36]J. Zheng, S. Zhai, D. Wu, and Y. Sun, "$S^+X^-I^+$ Route to Mesostructured Materials from Fau and Beta Zeolite Precursors: A Comparative Study of Their Assembly Behaviors in Extremely Acidic Media," *J. Solid Chem.*, **178**, 1630–6 (2005).

[37]S. Han, W. Hou, J. Xu, X. Huang, and L. Zheng, "Study of the *Pm3N* Space Group of Cubic Mesoporous Silica," *Chem. Phys. Chem.*, **7**, 394–9 (2006).

[38]M. C. Liu, H. S. Sheu, and S. Cheng, "Drying Induced Phase Transformation of Mesoporous Silica," *Chem. Commun.*, **23**, 2854–5 (2002). □